Proton Spin Relaxation and Molecular Motion in a Bulk Polycarbonate

Alan A. Jones* and John F. O'Gara

Department of Chemistry, Jeppson Laboratory, Clark University, Worcester, Massachusetts 01610

Paul T. Inglefield

Department of Chemistry, College of the Holy Cross, Worcester, Massachusetts 01610

John T. Bendler and Albert F. Yee

Polymer Physics and Engineering Branch, Corporate Research and Development Center, General Electric Company, Schenectady, New York 12301

K. L. Ngai

Naval Research Laboratory, Washington, D.C. 20375. *Received January 19, 1982*

ABSTRACT: Proton spin–lattice relaxation and proton spin–lattice relaxation in the rotating frame were observed in the solid polycarbonate of 1,1-dichloro-2,2-bis(4-hydroxyphenyl)ethylene from 150 to 400 K. This polymer is suited to this type of study since it contains only a single type of proton. The relaxation times are quantitatively interpreted as a function of temperature using a correlation function–spectral density approach. Two types of correlation functions that are somewhat successful result from the one-dimensional defect diffusion model (DDM) and the correlated states model (CSM). Both can adequately simulate the proton relaxation data but the CSM also successfully accounts for the temperature dependence of the second moment and accurately predicts the location and much of the width of the low-temperature mechanical loss peak. The activation energy of the fundamental process in the CSM is also close to that observed in dilute solutions of the same polycarbonate and close to that calculated by MNDO (modified neglect of diatomic overlap) applied to model compounds. The Hartree–Fock calculations in conjunction with the earlier proton line width study are used to consider the repeat unit level geometry of the motion causing both spin relaxation and mechanical loss.

Introduction

Examination of relaxation processes and molecular motion in aromatic polycarbonate glasses has been widespread and fruitful.[1-9] The presence of considerable molecular motion in these glasses and the high impact resistance of molded specimens under certain circumstances have attracted many investigators, including ourselves.

In an earlier proton line shape study[9] of the polycarbonate of 1,1-dichloro-2,2-bis(4-hydroxyphenyl)-ethylene, or chloral polycarbonate, the geometry of the predominant intramolecular motion affecting phenylene groups was clearly established as phenylene group rotation or rotational oscillation about or parallel to the 1,4 axis. At the time of the line shape study, the only motion put forth was simple phenylene group rotation but in this paper the prospect of other motions that preserve the orientation of the C_1C_4 axis is considered. The determination of geometric information from the line shape was expedited by the location of the principal intramolecular dipole–dipole interaction between the 2,3 protons of the phenylene ring parallel to the chain backbone (see Figure 1). Since there is essentially only a single type of proton in the chloral polycarbonate and since a detailed line shape study has already been completed, a proton spin relaxation study is reported here to characterize the time scale and energetics of the motion of the phenylene group.

To attain this goal with some certainty, proton spin–lattice relaxation times, T_1's, were measured at two Larmor frequencies, 20 and 90 MHz, over a temperature range from about 150 to 400 K. Spin–lattice relaxation times in the rotating frame, $T_{1\rho}$'s, were also added to these data over the same temperature range. Some complications and limitations are avoided in this single type of proton study, where there are no overlapping resonances and there is no spin diffusion to other types of protons. Also the dipolar field is much less than the applied radio-frequency field at all temperatures, the value of the motionally modulated second moment is already known, and a wide range of temperature and frequency is being examined.

A quantitative interpretation of these relaxation data is sought based on a homogeneous correlation function for motional modulation of the dipole–dipole interaction. If, as will be shown, the time scale and energetics can be quantified in a correlation function, it is natural to explore the possible relationship to the dynamic-mechanical studies on the glass. The temperature-dependent spectral densities obtained from the spin relaxation studies will be used to calculate the response at the temperature and frequency of the mechanical experiments. Again both the position of the loss peak and the shape of the loss peak will be of interest, and considerable success is found when the correlation function developed from spin relaxation is used.

However, the extent of mechanical activity due to a molecular relaxation depends on factors other than the amount of spectral density at the frequency of the applied stress. It is necessary that the motion produce a local strain in the solid. Thus the rotation of a symmetrical group such as CH_3 produces no mechanical loss in first order. The small loss peaks sometimes attributed to CH_3 arise from higher order terms in the stress or from a correlated motion of the rest of the molecule which produces a net strain. The mechanical loss peak at −100 °C at 1 Hz in polycarbonates, called the γ peak here, is quite large and is accompanied by a sizeable bulk component.[8] It is unlikely, then, that the motion causing this peak could arise from a symmetrical moiety hopping between equivalent sites. Such a motion or an oscillation in place would show little bulk loss.

Since both the NMR and mechanical studies suggest that the phenylene ring motion occurs in the solid, Hartree–Fock calculations were performed for model com-

0024-9297/83/2216-0658$01.50/0

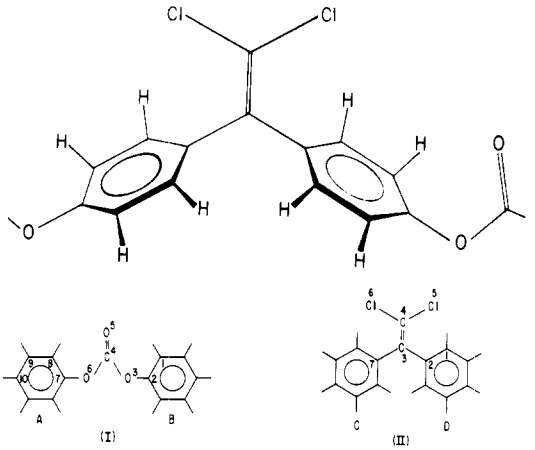

Figure 1. Structure of the repeat unit of the polycarbonate of 1,1-dichloro-2,2-bis(4-hydroxyphenyl)ethylene. Two model compounds used for calculations are diphenyl carbonate (I) and 1,1-dichloro-2,2-diphenylethylene (II).

pounds related to chloral polycarbonate. These calculations elucidate the nature of the conformational energy surfaces and provide a definitive link to the question of the geometry of the motion. The conformational energy surfaces can be compared to the results of solution NMR studies, where relaxation is dominated by intramolecular interactions; also one of the interpretational models used for bulk relaxation provides an activation energy for the fundamental process occurring in the glassy polymer.

Experimental Section

The chloral polycarbonate for this study was synthesized at General Electric and the intrinsic viscosity of the polymer was about 0.5 dL/g in methylene chloride. A carefully dried sample of powdered polymer was compression molded at 210 °C into a solid cylindrical plug 10 mm in diameter and 15 mm in height. The plug was allowed to cool to room temperature in the mold without quenching and was ground down to fit into a 10-mm glass NMR tube, where it was sealed under vacuum after vacuum drying.

Proton spin–lattice relaxation times were measured at Larmor frequencies of 20 and 90 MHz on a Bruker SXP 20-100 variable-field, multinuclear, FT NMR spectrometer. The $\pi/2$ pulse width was 2 μs and a standard $\pi-\tau-\pi/2$ pulse sequence was used with a cycle time greater than 10 times T_1. Proton spin–lattice relaxation times in the rotating frame were measured at a radio-frequency field strength of 1.0 mT using a standard $\pi/2$-phase-shifted locking pulse sequence. Temperature control was maintained to within ±2 K with a Bruker B-ST 100/70 temperature controller.

Results

The proton T_1 data at 20 and 90 MHz are well characterized by a linear least-squares analysis of ln $(A_\infty - A_\tau)$ vs. τ, where the A's are signal amplitudes and the τ's are delay times. No dispersion of relaxation times is observed and the T_1 data are summarized as a function of temperature in Figure 2. The uncertainty in a given T_1 value is ±10%.

The proton $T_{1\rho}$ data are again adequately characterized from a linear least-squares analysis of ln A_τ vs. τ as can be seen in Figure 3. Here, A is still signal amplitude but τ is now the length of the locking pulse. Since the deviations from simple exponential decay are small in Figure 3 and not indicative of a dispersion of relaxation times,[6,7] a fit of the whole curve to single-exponential decay is employed. These proton $T_{1\rho}$ data are also summarized in Figure 2 as a function of temperature, but the error is somewhat larger, ±15%, mostly reflecting the accuracy of setting the radio-frequency phase shift and the accuracy

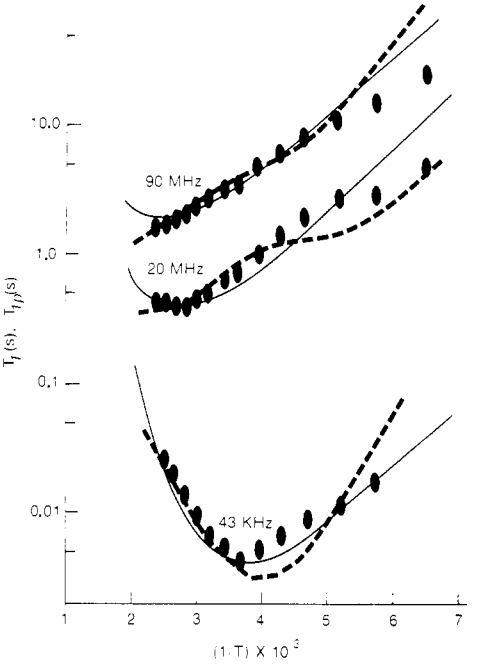

Figure 2. Spin–lattice relaxation time and the spin–lattice relaxation time in the rotating frame vs. inverse temperature. Dot size approximates experimental error. The dashed line corresponds to the best simulation of the relaxation behavior using eq 1–5, which are based on one-dimensional defect diffusion and a second, independent single-exponential process. The solid line corresponds to the best simulation of the relaxation using eq 1, 6, and 7, which are based on the correlated states model.

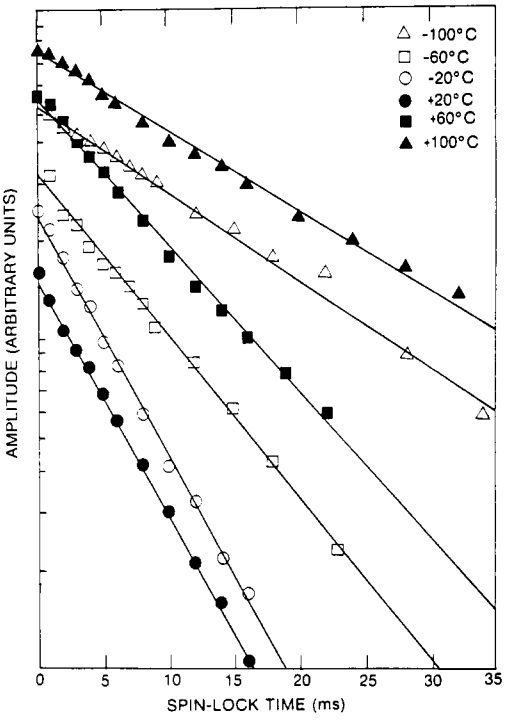

Figure 3. Amplitude of the signal vs. spin lock time.

of determining the radio-frequency field magnitude from successive maxima and nulls.

Interpretation

As discussed in the Introduction, the approach will be to write both T_1 and $T_{1\rho}$ as a function of spectral densities produced by motional modulation of the proton dipole–dipole interaction. A single correlation function and the associated spectral density will then be used to quantitatively simulate both T_1 and $T_{1\rho}$ as a function of temper-

ature. The standard T_1 and $T_{1\rho}$ expressions are[10,11]

$$1/T_1 = (2/3)\gamma^2 S[J_1(\omega_H) + 4J_2(2\omega_H)]$$
$$1/T_{1\rho} = (2/3)\gamma^2 S[1.5J_e(2\omega_e) + 2.5J_1(\omega_H) + J_2(2\omega_H)] \quad (1)$$

where $\omega_e = \gamma_H H_{rf}$ and S is the second moment.[9]

For a spectral density interpretation based on motional modulation of dipole–dipole interactions to be valid, spin diffusion must be negligible. Since there is only a single type of proton in the repeat unit and since the molecular mass of the polymer is high ($\sim 5 \times 10^4$ daltons), leaving few end groups, spin diffusion to another type of proton is unlikely. This is especially unlikely in this sample since there is also considerable molecular motion over most of the temperature range as evidenced by line narrowing[9] and quite short T_1's. Spin diffusion could be occurring to only a few motionally active phenylene groups but again the line shape is not indicative of a few active phenylene groups but rather shows the majority of the phenylene groups to be undergoing fairly substantial rotation or rotational oscillation about or parallel to the 1,4 axis above 220 K. There is little evidence of some few phenylene groups enjoying other degrees of freedom, which would lead to a narrow line on top of the observed broad line, though surely some phenylene groups could be rotating or oscillating with somewhat greater freedom than others in the glassy matrix. On the other hand, since the line shape, T_1, and $T_{1\rho}$ data do not display such sample heterogeneity, it shall not be included in the interpretation. A limited heterogeneity could be averaged by spin diffusion among the phenylene protons. For this polycarbonate, T_2 is of the order of 100 μs, which would allow for spin exchange among protons on a few phenylene groups in, say, the first millisecond of the $T_{1\rho}$ decay. This might be sufficient to obscure some heterogeneity but not a large heterogeneity. In the absence of evidence for a significant heterogeneity, a homogeneous correlation function will be used with the qualification that limited heterogeneity may be present.

The applicability of a spectral description for $T_{1\rho}$ also requires that $H_{rf}^2 \gg H_L^2$, where H_L is the local dipolar field. This is one of the strong points of this particular investigation since the large distances between phenylene protons result in a small H_L. Using the relation $H_L^2 = {}^1/_3 S$, one finds that even in the rigid-lattice limit, S equals 0.046 mT^2 and therefore H_L^2 equals only 0.015 mT^2. Thus in our case, with H_{rf}^2 equal to 1 mT^2, the condition $H_{rf}^2 \gg H_L^2$ is valid even in the low-temperature, rigid-lattice limit and then becomes increasingly favorable as temperature is raised.

For both T_1 and $T_{1\rho}$ below temperatures of about 220 K, an approach based on motional modulation of the dipole–dipole interaction may begin to fail since motion will eventually become too slow. Therefore we can anticipate the largest discrepancies between the interpretation and the data to be at the lowest temperatures. However, we do have data over a 200 K range above 220 K, leaving a substantial data base for interpretation.

The value of S, the second moment, employed in eq 1 should correspond to the motionally modulated component of the second moment characterized in the earlier line shape study.[9] This motionally modulated dipole–dipole interaction corresponds to part of the intermolecular dipole–dipole contributions since the predominant motion causing modulation is phenylene group rotation or rotational oscillation, which does not reorient the largest intramolecular dipole–dipole interaction. By and large, S is not given an explicit temperature dependence except through the spectral density, and, from that viewpoint, S will be compared with the spectral density near zero frequency.

If we are to employ a spectral density approach and have some knowledge of S, the main interpretational problem remaining is to develop a temperature-dependent expression for the spectral density or, equivalently, the correlation function. The temperature dependence will be introduced through an assumed Arrhenius dependence for the correlation times or times in any expression for the spectral density or correlation function. In those cases where there are adjustable parameters both for the correlation times and for the distribution of correlation times, no temperature dependence of the distribution will be invoked. This is just a simplification but it is preferable if we can account for the temperature dependence of the relaxation.

Within this general approach of a known motionally modulated S, Arrhenius behavior for correlation times, and a temperature independence of parameters controlling the distribution of relaxation times, we can begin to try to account for the data in Figure 2. A single-exponential correlation function[12] is inadequate since it cannot account for the frequency dependence or the temperature dependence at one frequency. Models involving two-exponential correlation functions such as the Woessner model[13] are inadequate for similar reasons. Models involving various mathematical distributions of exponential correlation times employed by others to interpret spin relaxation were tried, including rectangular,[14] Cole–Cole,[15] log χ^2,[16] and Fuoss–Kirkwood[17] models, and were found not to account for the shape as a function of temperature.

The first traditional model that was somewhat successful in our hands is based on one-dimensional defect diffusion. In the final analysis, this approach fails to meet the goals of this paper. It is only included here to show the lengths taken to try to account for the data with conventional models. The basic function is

$$\phi_{DD}(\tau_D) = \exp(\tau/\tau_D)\ \mathrm{erfc}\ (\tau/\tau_D)^{1/2} \quad (2)$$

where τ_D is the defect diffusion correlation time, which is assumed to have an Arrhenius behavior.

$$\tau_D = \tau_D^{\infty} \exp(E_A^{DD}/RT) \quad (3)$$

Actually the defect diffusion equation alone describes only the high-temperature region and the addition of a second process characterized by a single-exponential correlation time, τ_0, is required to match the low-temperature behavior. We shall denote the single-exponential correlation time correlation function[12] as ϕ_{BPP}; then the product correlation function is written as

$$\phi = \phi_{DD}(\tau_D)\phi_{BPP}(\tau_0) \quad (4)$$

where

$$\phi_{BPP} = \exp(-\tau/\tau_0)$$
$$\tau_0 = \tau_0^{\infty} \exp(E_A^{\circ}/RT)$$

To allow for the most general situation, the actual correlation function used to account for the data is written as

$$\phi(t) = (A + B\phi_{BPP})(C + D\phi_{DD}) = AC + BC\phi_{BPP} + BD\phi_{DD}\phi_{BPP} + AD\phi_{DD} \quad (5)$$

This form provides for all cases from modulation of independent second-moment contributions by the two processes to modulation of the same second-moment contribution by the two processes. If $\phi(t)$ is normalized to 1 at

$t = 0$, then AC corresponds to the fraction of S that is not motionally modulated and $BC + BD + AD$ corresponds to the fraction of S that is motionally modulated. Furthermore, BC corresponds to the fraction modulated by the BPP process only, AD to the fraction modulated by the direct diffusion process only, and BD to the fraction modulated by both processes. The fraction AC and the sum $BC + BD + DD$ can be compared directly with the results of the line shape analysis.

The spectral densities or Fourier transforms of ϕ_{BPP}, ϕ_{DD}, and $\phi_{BPP}\phi_{DD}$ are all known and the components of the second moment associated with the various processes described by the fractions AC, BC, BD, and AD can be labeled S_A, S_{BPP}, $S_{BPP\text{-}DD}$, and S_{DD}, respectively. These spectral densities and second moments can then be substituted in eq 1 to calculate T_1's and $T_{1\rho}$'s. The values of these S's, τ_0^∞, τ_D^∞, $E_A°$, and E_A^{DD} are then adjusted to produce the best simulation of the data (Figure 2). The values of the model parameters producing the simulation are $S_A = 3.0 \times 10^{-2}$ mT^2, $S_{DD} = 1.1 \times 10^{-2}$ mT^2, $S_{BPP} = 0.092 \times 10^{-2}$ mT^2, $E_A^{DD} = 34$ kJ, $E_A° = 11.2$ kJ, $\tau_D^\infty = 1 \times 10^{-13}$ s, $\tau_0^\infty = 5 \times 10^{-12}$ s, and $S_{BPP\text{-}DD} = 0.034$ mT^2.

The values of S are consistent with the line shape analysis. The change in S between the rigid-lattice value and just before T_g is 1.5 ± 0.4 while the sum $S_{DD} + S_{BPP\text{-}DD} + S_{BPP} = 1.2$; the value of S in the high-temperature limit just before T_g is 3.1 ± 0.2, which compares well with S_A.

The stimulation of the data as shown in Figure 2 is adequate at high temperatures (above about 250 K), with the largest deviations at low temperatures. This is consistent with the limitations of the spectral density approach. The defect diffusion process modulating a second moment of 1.1×10^{-2} mT^2 is the principal process. The low-temperature BPP process modulates much less second moment though it is necessary to avoid extremely large deviations between the simulation and the data at low temperatures. In terms of connecting these two relaxation processes to a molecular level description, the main process of defect diffusion is associated with cooperative phenylene ring rotation or reasonably large amplitude rotational oscillation. This is the predominant intramolecular motion deduced from line shape analysis.[9] The second minor process described by a BPP correlation function might be low-amplitude vibration though neither relaxation time nor line shape data can definitely characterize this since so little second moment is involved.

However, we could employ a more realistic description of the low-amplitude motion in the correlation function by replacing ϕ_{BPP} with a correlation function specifically developed to describe low-amplitude motion short of passage over a barrier. For this case, angular excursions would be about ±15° or less while large-amplitude motion over a barrier will be continued to describe one-dimensional defect diffusion. Gronski[23,24] has developed an appropriate correlation function for restricted rotation, but combining this result with the DDM produced an interpretation about as good as the one just displayed so it will not be presented.

In all fairness, the DDM simulation of T_1 and $T_{1\rho}$ is heavily parametrized. Furthermore, efforts to extend this interpretation to the temperature dependence of S and the mechanical loss fail nearly completely. Thus, though the DDM is the most successful of the conventional correlation functions in our hands, it falls well short of the goal of a quantitative interpretation of spin relaxation and mechanical loss.

A second, fundamentally different model that proves more capable corresponds to a fractional exponential correlation function proposed by others on empirical grounds[26,27] and developed by one of us (K.L.N.) on the basis of correlated state excitations in condensed matter.[28-30] It is referred to herein as the correlated state model (CSM). The correlation function is

$$\phi(t)_{CSM} = \phi(0) \exp[-(t/\tau_p)^{1-n}] \tag{6}$$

where $0 < n < 1$ and the loss peak frequency is located at $\omega_p \propto \tau_p^{-1}$, where

$$\tau_p = [(1 - n)e^{n\gamma}E_c^{\,n}\tau_0]^{1/(1-n)} \tag{7}$$

with $\tau_0 = \tau_\infty \exp(E_A/RT)$, the microscopic correlation time, E_c the bath cutoff energy, and $\gamma = 1.577$ Euler's constant. As set forth in eq 6 and 7, the CSM has four parameters, τ_∞, E_A, n, and E_c. The first two fix the microscopic dynamics and energetics of the fundamental process in the absence of strong correlations; n and E_c determine the width of frequency dispersion and the renormalized time scale due to medium effects. When $n \neq 0$, τ_p is quite different from τ_0 and $\tau_p = \tau_\infty^* \exp(E_A^*/RT)$, where E_A^* is the apparent activation energy, given by $E_A^* = E_A/(1 - n)$ and the apparent preexponential: $\tau_\infty^* = [(1 - n)\cdot \exp(n\gamma)E_c^{\,n}\tau_\infty]^{1/(1-n)}$. Figure 2 shows the fit of the CSM spectral density to the chloral polycarbonate T_1's and $T_{1\rho}$, using the parameters $E_A = 10$ kJ/mol, $n = 0.8$, and $\tau_\infty^* = 2.29 \times 10^{-16}$ s. Even though fewer parameters are used than for DDM (defect diffusion model), the agreement with experiment seems superior.

The physical picture connecting the CSM to motion in chloral polycarbonate begins with identifying the fundamental process as phenylene group rotation or rotational oscillation. This fundamental process could be detected in the absence of strong matrix effects in dilute solution but a value of $n = 0.8$ indicates that in the bulk glass the fundamental process is strongly affected by the medium. The activation energy in the absence of medium effects is 10 kJ and the apparent activation energy in the glass is substantially larger, 50 kJ, reflecting the strong medium influence. The apparent preexponential τ_∞^* is too short to be a physically sensible preexponential itself. However, in the CSM, the true preexponential τ_∞ could be substantially longer and thus fall into a physically reasonable region. A knowledge of E_c is required to calculate τ_∞, but, with the solid chloral data in hand, E_c and τ_∞ cannot be separately determined—only the composite quantity τ_∞^* can be obtained.

It is perhaps worthwhile to point out that an equally good account would be given by the "alternative" Williams/Watts[26] correlation function:

$$\phi_{WW}(t) = \phi(0) \exp[-(t/\tau^{WW})^\beta] \tag{8}$$

with $\beta = 0.2$, $\tau^{WW} = \tau_\infty^{WW} \exp[E^{WW}/RT]$, $\tau_\infty^{WW} = 2.29 \times 10^{-16}$ s, and $E^{WW} = 50$ kJ/mol. It is in fact apparent that eq 6 and 8 are mathematically identical and that the difference consists in the interpretation of the parameters. In the Williams/Watts picture, β, E^{WW}, and τ_∞^{WW} are unrelated. In the case of CSM, E_A and τ_∞ are renormalized by n and E_c but approach their isolated values as $n \to 0$.

The largest deviation between the CSM fit and the data occurs at low temperatures, where in the case of the DDM we added terms for low-amplitude oscillation. These terms could be combined with the CSM but the complexity of the mathematics has prevented completion of this task. The amount of motionally modulated second moment employed in the CSM fit is 2.0×10^{-2} mT^2. This is somewhat larger than the experimental value of $(1.5 \pm 0.4) \times 10^{-2}$ mT^2 observed at the highest temperatures of the study. However, the CSM fitting value could be somewhat

larger since it corresponds to a very broad distribution of exponential correlation times, some of which could be too large to contribute to line narrowing even at the higher temperatures of the experimental study.

A direct interpretation of the line narrowing study reported earlier[9] can be made by using the CSM spectral density expression developed here. This can be made as a test without further parameter adjustment and will employ the spectral density expression around zero frequency, already developed to account for T_1 and $T_{1\rho}$ at higher frequencies. The dependence of the line width, $\delta\nu$, on the spectral density in a motionally narrowed situation can be written[12]

$$(\delta\nu)^2 = (3/16\pi^2)\gamma^4\hbar^2 I(I+1)\int_{-\xi\delta\nu}^{+\xi\delta\nu} J_0(\nu)\,\mathrm{d}\nu \qquad (9)$$

The constant ξ is of the order of unity and it arises from uncertainties in the integration limits and from inaccuracies in the definition of $\delta\nu$.

In order to avoid these uncertainties we will use a relative second moment (S/S_{RL}), where S_{RL} is the rigid-lattice second moment, as a measure of $(\delta\nu)^2$ and derive an expression for the dependence of this parameter on the spectral densities $J_0(\nu)$ integrated over the frequency range near zero corresponding to the overall line width range ($\delta\nu$).

We have from eq 9

$$S = Z\int_{-\delta\nu}^{+\delta\nu} J_0(\nu)\,\mathrm{d}\nu \qquad (10)$$

where Z is the preintegral factor in eq 9 and contains any proportionality constants between S and $(\delta\nu)^2$.

Now

$$S_{RL} = \int_{-\delta\nu}^{+\delta\nu} J_0(\nu)\,\mathrm{d}\nu \quad \text{in the limit } \tau \to \infty$$
$$= ZI \qquad (11)$$

If, as in the general case, part of the rigid-lattice second moment is unmodulated and not narrowed by the motion, then eq 10 becomes

$$S = A^2 + Z\int_{-\delta\nu}^{+\delta\nu} J_0(\nu)\,\mathrm{d}\nu \qquad (12)$$

where A^2 is that part of the second moment unaffected by the motion.

Combining eq 11 and 12 yields

$$\frac{S}{S_{RL}} = \frac{A^2}{ZI} + \frac{\int_{-\delta\nu}^{+\delta\nu} J_0(\nu)\,\mathrm{d}\nu}{I} \qquad (13)$$

which may be written as

$$S/S_{RL} = a + m\int_{-\delta\nu}^{+\delta\nu} J_0(\nu)\,\mathrm{d}\nu$$

where a and m are constants and the integration is carried out over the frequency range of the absorption line. Equation 13 has a form identical with that used by Gutowski and Pake for an exponential correlation function to analyze motion in solid 1,1,1-trichloroethane. Numerical evaluation of the $J_0(\nu)$'s over the spectral range of interest ($\pm\delta\nu$) for a given correlation function will thus permit the evaluation of the integral in eq 13. With the temperature-dependent spectral densities developed to account for T_1 and $T_{1\rho}$, the observed temperature dependence of S can be interpreted with eq 13.

The spectral densities at each temperature corresponding to the second-moment data[9] are evaluated numerically by using a fast Fourier transform program with the CSM correlation function (eq 7) with $n = 0.8$ and the τ_p's calculated for an Arrhenius temperature dependence with $\tau_\infty^* = 2.29 \times 10^{-16}$ s and $E_A^* = 50$ kJ/mol (the parameters used to account for the T_1 and $T_{1\rho}$ data). The integrals in eq 13 are evaluated over the spectral range of interest (±20 kHz) and a reasonable fit to the reduced experimental second moments (S/S_{RL}) over the temperature range of interest is obtained with $a = 0.648$ and $m = 0.022$ in eq 14. This fit is illustrated in Figure 4. It should be noted that the temperature dependence of $\int J_0(\nu)\,\mathrm{d}\nu$ evidences the same general shape as the second-moment data, remaining constant below about 200 K, i.e., in the rigid-solid, long-τ_p region, where the expected frequency range of the spectral density is very narrow. Also, the continued slow decrease in second moment at higher temperatures is accounted for by the model.

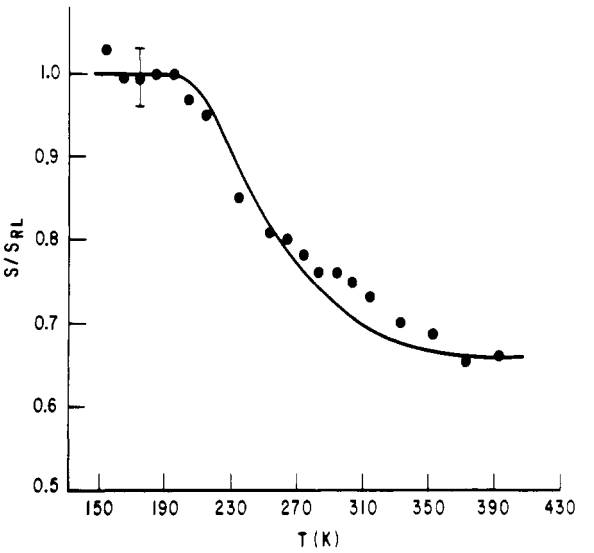

Figure 4. Second moment vs. temperature. The solid line is a simulation using eq 6, 7, and 13, which are based on the correlated states model. The model parameters are the same as those used to produce the CSM simulation in Figure 2.

The successful simulation of the temperature dependence of S with an apparent activation energy of 50 kJ/mol contrasts with the earlier interpretation[9] using the Bray–Hendrickson analysis, which showed the presence of two processes with significantly differing activation energies, 20 and 4 kJ/mol. The discrepancy between the CSM result and the earlier analysis may only result from the limitations of the simplistic approach originally applied. Also, while the CSM interpretation is fairly consistent with the second-moment data, the model parameters could not be determined from the second-moment data alone. It can also be briefly noted again that the defect diffusion model does not lead to a reasonable simulation of the temperature dependence of S using this same approach.

Comparison with Mechanical Relaxation

Having found a reasonable description of the spin relaxation results which also accounts for the temperature dependence of S, we turn now to the mechanical loss studies to see whether the same underlying process might be responsible.

Low-temperature mechanical loss peaks have been studied for many polycarbonates[8,31] and attention usually focuses on the very large dispersion located at about −100 °C at 1 Hz, which we call the γ peak.[8] The γ peak in chloral polycarbonate has been measured by one of us[8] (A.F.Y.), and the attempt is therefore made to see if the correlation functions used for the magnetic relaxation data can also account for the γ peak. It is well-known[32] that

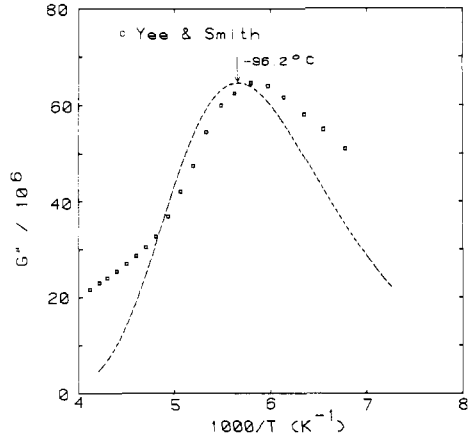

Figure 5. Dynamic mechanical spectrum. The dashed line is the simulation employing eq 16 and the correlated states model parameters used to produce the simulations of NMR data in Figures 2 and 4.

the frequency-dependent moduli of a solid are given by the Fourier transform of the autocorrelation of the appropriate stresses. Therefore, for the shear modulus G

$$G(\omega) = \frac{1}{k_\beta T}\int_0^\infty e^{i\omega t}\langle -\dot{\sigma}_G(t)\sigma_G(0)\rangle \, dt \qquad (14)$$

where σ_G is the shear stress and the angular brackets denote the ensemble average. If the molecular motion seen in the spin relaxation experiments is also stress sensitive, then part of the instantaneous stress can be relaxed by the "phenylene-type" motion as described by the previous correlation functions. Thus

$$G_\gamma(\omega) = \frac{\langle \sigma_\gamma(0)^2\rangle}{k_\beta T}\int_0^\infty e^{i\omega t}[-\phi'(t)] \, dt \qquad (15)$$

where G_γ is the part of the shear modulus relaxed by the motion, σ_γ is the stress arising from the molecular changes, and $\phi'(t)$ is the derivative of either the DDM or CSM correlation function $\phi(t)$. The mechanical loss $G_\gamma(\omega)^{loss}$ is given by the imaginary part of eq 15:

$$G_\gamma(\omega)^{loss} = \frac{\langle \sigma_\gamma(0)^2\rangle}{k_\beta T}\int_0^\infty \sin(\omega t)\phi'(t) \, dt \qquad (16)$$

The defect diffusion correlation function with the parameters determined from fitting the T_1 and $T_{1\rho}$ data can be used to predict a mechanical loss peak using eq 17 and the appropriate frequency for the mechanical measurement,[8] 1 Hz. The observed loss peak is at −100 °C and the predicted peak is at −125 °C, using the defect diffusion parameters derived when the low-temperature, low-amplitude process is described by a BPP correlation function.

This prediction is not very good. However, the results of computing eq 16 for the CSM at the temperature and frequency of the measurements in ref 8 are shown in Figure 5. In Figure 6 is the relaxation map constructed with the T_1 minima, the $T_{1\rho}$ minimum, and the mechanical loss peak. It is seen that the NMR minima and mechanical loss peaks are quite consistent with an apparent activation energy of 50 kJ/mol. The shape as well as the position of the mechanical loss peak is fairly well predicted. The magnitude of the calculated loss peak is controlled by $\langle \sigma(0)^2\rangle$, which is adjusted to match the data in Figure 5. The observed loss peak is broader than the prediction though the γ loss peak has been said to be composed of up to three peaks.[8] The phenylene ring motion characterized by NMR appears to be at least one of these peaks and is located near the position of greatest loss.

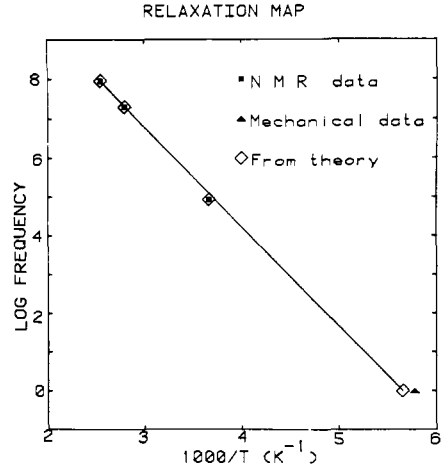

Figure 6. log (frequency)–inverse temperature grid or relaxation map.[28-30] The NMR minima and the mechanical loss peak maximum are plotted on a frequency–temperature grid. The frequency is characteristic of the experiment and the temperature is that of the minimum or maximum. The solid line corresponds to the 50 kJ/mol activation energy used to produce the simulation in Figure 2. The 20-MHz T_1 minimum and the $T_{1\rho}$ minimum are fairly well located by the data but the position of the 90-MHz T_1 minimum is only a rough estimate.

Taken together with other evidence in the literature,[2-9] the results of Figures 2, 4, 5, and 6 are a rather convincing indication of the connection between the spin relaxation and the mechanical relaxation measurements. As mentioned in the Introduction, the participation of the "phenylene ring" motion in a mechanical loss process poses interpretational problems from the molecular standpoint, which are partially addressed in the next section.

Hartree–Fock Calculations for Chloral Polycarbonate Models

The discovery[9] that the molecular motion in glassy chloral polycarbonate which diminishes the second moment also preserves the angle which the 1,4-phenylene axis makes with the applied field sharply reduced possible molecular conformational interpretations. Since the second-moment study[9] and the present spin relaxation study are both looking exclusively at the ring proton motion, it must be concluded that the dynamics described by the time correlation functions likewise preserves the orientation of the 1,4 axis.

Rather subtle chemical modification of the polycarbonate structure sometimes results in dramatic changes in bulk mechanical properties.[4,8] Partly for this reason one of us (J.T.B.) undertook empirical and quantum calculations on model compounds related to polycarbonate.[33] These calculations support the earlier findings of Tonelli[34] that phenylene ring motion occurs quite easily, both at the carbonate unit (~13.0 kJ/mol activation energy using MNDO) and at the isopropylidene unit in BPA–PC (the activation energy is 13.8 kJ/mol at the *gem*-dimethyl side according to molecular mechanics).[6]

In light of the present results, suggesting that the motion seen in the magnetic and mechanical relaxation is identical or closely related, we decided to repeat these calculations for the model compounds of chloral polycarbonate: diphenyl carbonate (I) and 1,1-dichloro-2,2-diphenylethylene (II) (Figure 1).

The earlier study of I using MNDO[35] showed that the most stable form had both rings A and B perpendicular to the plane of the carbonate unit, with both ring–oxygen bonds 2–3 and 7–6 in the plane of the carbonyl unit 4–5. As the A ring–carbonate dihedral angle 8–7–6–4 is moved

away from 90° to 0° and then to −90°, an activation of 13.8 kJ/mol is encountered and the 7–6 bond is driven to the trans position with respect to the carbonyl. (All results are for complete geometrical optimization.) The activation energy for this lowest energy motion of the 8–7–6–5 ring dihedral angle past the carbonate group is in reasonable accord with the "microscopic" E_A found for the CSM fit after eq 6 and for the solution activation energy for phenylene ring motion.[36] There are, though, two problems with the result. First, the X-ray crystal data indicate that the equilibrium value of the dihedral angle 8–7–6–4 is nearer to 60° than 90°.[37] Second, the direction of the phenylene axis, connecting atoms 7 and 10, is moved through nearly 87° by this conformational change, in contradiction to the glassy-state second-moment results,[9] which require that the direction of this axis be at least nearly preserved.

We decided, therefore, to repeat the study of I, this time looking at the direct isomerization involving the cis/trans dihedral angle 7–6–4–5 and using MNDO and the ab initio Hartree–Fock program GAUSSIAN 80[38] at the STO-3G minimal basis level. The activation energy for the 7–6–4–5 motion given by MNDO (10 kJ/mol) is in reasonable agreement with the E_A of the CSM fit (see eq 7 and 8) and the solution results.[36] The GAUSSIAN 80 activation energy is about twice as large (22 kJ/mol) as the MNDO value or the experimental result. This difference may be due to the minimal basis set (STO-39) or incomplete geometrical optmization. In addition, GAUSSIAN 80 gives 8–7–6–5 about 66° (and therefore closer to the X-ray result).[37] Another significant aspect of the calculated cis/trans isomerization is that it nearly retains the spatial orientation of the C_1C_4 phenylene axis. An axis of rotation inclined by 15° or less from the C_1C_4 axis would not be experimentally distinguishable from simple phenylene rotation by the line shape study, and this condition is met by the calculated cis/trans isomerization.

To compare this segmental motion with simple ring rotation in chloral polycarbonate, an MNDO calculation was performed on the dichloroethylene unit in II, which yielded a barrier of 42 kJ. On this basis, simple rotation about the C_1C_4 axis seems less likely in chloral than in BPA and less likely than the cis/trans isomerization. However, a larger portion of chain should be considered in evaluating the isomerization as well as translation of the ends of the portion following isomerization before this assignment is made. Also both the isomerization and the rotation calculation were made for complete motions and not for oscillations though reasonably large amplitude oscillations could account for our NMR data.

Other recent deuterium[39] and carbon-13 results[40,41] indicate simple 180° ring flips and ring oscillation in BPA polycarbonate, and, because of the simplicity of these motions, they are still attractive possibilities for chloral. At this time, our results do not decisively distinguish between simple rotation and cis/trans isomerization or the amplitude of either motion.

Conclusions

The proton relaxation times determined in this structurally specific, single type of proton study provide a suitable basis for a quantitative description employing a correlation function–spectral density approach. The same spectral density reflecting the same motions accounts for both T_1 and $T_{1\rho}$. The observation of spin relaxation over a wide range of frequency and temperature provides a test of potential interpretations; however, two were found to be at least somewhat satisfactory. The first model, based on one-dimensional defect diffusion, is barely adequate while the second model, based on correlated states, is better, especially since it reproduces the asymmetric dependence of $T_{1\rho}$ on temperature around the $T_{1\rho}$ minimum and accounts for the temperature dependence of S.

Both the DDM and the CSM were used to predict the position and shape of the dynamic mechanical loss peak. Again the CSM is more successful in predicting the location of the loss peak as a function of temperature close to experimental error while the DDM misses by about 25°. The breadth of the loss peak is also fairly well described by the CSM though it appears there may be motions contributing to mechanical loss in addition to those which affect the phenylene protons as determined by spin relaxation.

With regard to the CSM, the values of the model parameters are physically sensible. The activation energy of the fundamental process, E_A, is 10 kJ, which is close to the dilute solution value[36] for phenylene rotation of 15 kJ. The same geometrical restrictions apply in solution as in the solid so the same dynamic process should be under consideration. The solution activation energy should be slightly higher than E_A since even in a 10 wt % solution the surroundings will affect the fundamental process. The value of 0.8 for n in the glass indicates a strong interaction of the surroundings with the fundamental process.

The MNDO calculations also give a comparable barrier of 10 kJ/mol for the cis/trans isomerization about the C–O bond connecting the carbonate and phenylene groups in diphenyl carbonate. This is a motion which should at least be considered as an alternative to simple ring rotation in chloral polycarbonate since it meets geometrical requirements indicated by the proton line shape study. Our current considerations leave both as possibilities, and either motion could also be present in the form of a fairly large amplitude oscillation short of complete rotation or isomerization.

It should be added that any other motion contributing to the broad γ mechanical loss peak seems likely to be somehow related to the phenylene group motion since the loss peak and the frequency–temperature superposition of phenylene group motion are both derived from NMR. Such other motions might contribute more to mechanical activity than a symmetric motion of the phenylene group, yet superposition argues for some relationship.

Acknowledgment. We thank Mr. Francis P. Shea for assistance in the operation of the NMR spectrometer and Mr. Joseph S. Fragala for assistance in computer calculations. The research was carried out with financial support of the National Science Foundation, Grant DMR-7906777, Polymers Program. This research was also supported in part by National Science Foundation Equipment Grant No. CHE 77-09059. K.L.N. acknowledges partial support by ONR, Task NR 318-059.

References and Notes

(1) Some recent, representative investigations of polycarbonates are given in ref 2–9 though this is not intended as an exhaustive survey.
(2) Pochan, J. M.; Ginson, H. W.; Froix, M. F.; Hinman, D. F. *Macromolecules* **1978**, *11*, 165.
(3) Garfield, L. J. *J. Polym. Sci., Part C* **1970**, *30*, 551.
(4) Massa, D. J.; Rusanovsky, P. P. *Polym. Prepr., Am. Chem. Soc., Div. Polym. Chem.* **1976**, *17* (2), 184.
(5) Davenport, R. A.; Manuel, A. J. **1977**, *18*, 557.
(6) Schaefer, J.; Stejskal, E. O.; Buchdahl, R. *Macromolecules* **1977**, *10*, 384.
(7) Steger, T. R.; Schaefer, J.; Stejskal, E. O.; McKay, R. A. *Macromolecules* **1980**, *13*, 1127.
(8) Yee, A. F.; Smith, S. A. *Macromolecules* **1981**, *14*, 54.
(9) Inglefield, P. T.; Jones, A. A.; Lubianez, R. P.; O'Gara, J. F. *Macromolecules* **1981**, *14*, 288.

(10) Solomon, I. *Phys. Rev.* **1955**, *94*, 559.
(11) Jones, G. P. *Phys. Rev.* **1966**, *148*, 332.
(12) Bloembergen, N.; Purcell, E. M.; Pound, R. V. *Phys. Rev.* **1948**, *73*, 679.
(13) Woessner, D. E.; *J. Chem. Phys.* **1962**, *30*, 1.
(14) McCall, D. W.; Douglas, D. C.; Anderson, E. W. *J. Chem. Phys.* **1959**, *30*, 1272.
(15) Heatley, F.; Began, A. *Polymer* **1970**, *17*, 399.
(16) Schaefer, J. *Macromolecules* **1973**, *6*, 882.
(17) Ghesquiere, D.; Ban, B.; Chachaty, C. *Macromolecules* **1977**, *10*, 743.
(18) Glarum, S. H. *J. Chem. Phys.* **1960**, *33*, 639.
(19) Hunt, B. I.; Powles, J. G. *Proc. Phys. Soc.* **1966**, *88*, 513.
(20) Valeur, B.; Jarry, J. P.; Geny, F.; Monnerie, L. *J. Polym. Sci., Polym. Phys. Ed.* **1975**, *13*, 667.
(21) Valeur, B.; Monnerie, L.; Jarry, J. P. *J. Polym. Sci., Polym. Phys. Ed.* **1975**, *13*, 675.
(22) Valeur, B.; Jarry, J. P.; Geny, F.; Monnerie, L. *J. Polym. Sci., Polym. Phys. Ed.* **1975**, *13*, 2251.
(23) Gronski, W.; Murayama, N. *Makromol. Chem.* **1978**, *179*, 1521.
(24) Gronski, W. *Makromol. Chem.* **1979**, *180*, 1119.
(25) Gutowsky, H. S.; Pake, G. E. *J. Chem. Phys.* **1950**, *18*, 162.
(26) Williams, G.; Watts, D. C. *Trans. Faraday Soc.* **1970**, *66*, 80.
(27) For a history of the fractional exponential function going back to Kohlrausch (1866) see: Struik, L. C. E. Abstracts of 10th Europhysics Conference on Macromolecular Physics, 1980, p 135.
(28) Ngai, K. L. *Comments Solid State Phys.* **1979**, *9*, 127–147.
(29) Ngai, K. L.; White, C. T. *Phys. Rev. B* **1979**, *20*, 2475.
(30) Ngai, K. L. *Phys. Rev. B* **1980**, *22*, 2066.
(31) McCrum, N. G.; Read, B. E.; Williams, G. "Anelastic and Dielectric Effects in Polymeric Solids"; Wiley: London, 1967.
(32) See: DeVault, G. P.; McClennan, J. A. *Phys. Rev.* **1965**, *137*, A724. Zwanzig, R. *J. Chem. Phys.* **1965**, *43*, 714.
(33) Bendler, J. T. *Ann. N.Y. Acad. Sci.* **1981**, *371*, 299.
(34) Tonelli, A. E. *Macromolecules* **1972**, *5*, 558.
(35) Dewar, M. J.; Thiele, W. *J. Am. Chem. Soc.* **1977**, *99*, 4899.
(36) O'Gara, J. F.; Desjardins, S. G.; Jones, A. A. *Macromolecules* **1981**, *14*, 64.
(37) Erman, B.; Marvin, D. C.; Flory, P. J. *Bull. Am. Phys. Soc.* **1981**, *26*, 227.
(38) Binkley, J. S.; Whiteside, R. A.; Kirshnan, R.; Seeger, R.; DeFrees, D. J.; Schlegel, H. B.; Topoil, S.; Kahn, L. R.; Pople, J. A. *QCPE* **1980**, *No. 406*.
(39) Spiess, H. W. International Union of Pure and Applied Chemistry, 28th Macromolecular Symposium Proceedings, 1982, p 35.
(40) Schaefer, J.; Sefcik, M. D.; Stejskal, E. O.; McKay, R. A.; Dixon, W. T., ref 39, p 25.
(41) Garroway, A. N.; Ritchey, W. M.; Moniz, W. B., ref 39, p 1.

Thermal and Mechanical Properties of a Poly(ethylene oxide-*b*-isoprene-*b*-ethylene oxide) Block Polymer Complexed with NaSCN

C. Robitaille and J. Prud'homme*

Department of Chemistry, University of Montreal, Montreal, Quebec, Canada H3C 3V1.
Received August 30, 1982

ABSTRACT: The changes in thermal and mechanical properties produced by complexation with NaSCN of a poly(ethylene oxide-*b*-isoprene-*b*-ethylene oxide) (PEO–PI–PEO) block polymer are described. The number-average molecular weight of the PEO–PI–PEO polymer was 1.67×10^5, and its PEO weight fraction was 0.14. It is shown that complexation, which occurs selectively with the PEO end blocks, can yield a semicrystalline thermoplastic elastomer that melts at about 450 K. The main characteristics of the complexed block polymer are a crystallization temperature, which occurs 90 K lower than that of complexed homo-PEO, and good dimensional stability at high temperature. However, the tensile strength of the complexed material appears to be considerably reduced with increasing temperature. A pronounced supercooling was also observed for the uncomplexed PEO–PI–PEO block polymer. This phenomenon seems to be a general feature of two-phase block polymers in which the crystallizable component is finely dispersed into isolated microdomains.

Introduction

Elastomeric ABA block polymers with crystalline end blocks have received increasing interest during the last decade.[1–7] Most investigations dealing with this class of block polymers have been oriented toward the development of novel thermoplastic elastomers possessing mechanical properties that compare favorably with those of the more conventional completely amorphous ABA block polymers, such as styrene–diene three-block polymers, but having a better dimensional stability at high temperature and/or a better resistance to solvents. Typical examples of such materials are those based on poly(ethylene sulfide),[1] polypivalolactone,[4] and hydrogenated 1,4-polybutadiene[5,6] end blocks. Also reported in the literature are data concerning ABA materials based on polythiacyclobutane[2] (PTCB) and poly(ethylene oxide)[3] (PEO) end blocks. Though the melting temperatures of PTCB and PEO are not high enough for considering elastomeric applications of the block polymers, these latter materials, which dissolved in aromatic solvents at moderate temperature, were good model systems for studying the role of the casting solvent and temperature on the morphology of the crystalline microdomains in specimens prepared by solvent casting.[2,3] In both cases it was shown that well-defined spherical or cylindrical crystalline microdomains were formed when the casting solvent and temperature were such that liquid–liquid phase separation occurred before crystallization.[2,3]

In the present paper, we describe the changes in physical and mechanical properties produced when a poly(ethylene oxide-*b*-isoprene-*b*-ethylene oxide) (PEO–PI–PEO) block polymer having a number-average molecular weight of 1.67×10^5 and a PEO weight fraction of 0.14 is complexed with NaSCN. It is known that PEO forms crystalline ionic complexes with a range of compounds including alkali metal and ammonium salts.[8–10] Wright[8] reported that ammonium, potassium, and sodium thiocyanate form crystalline complexes with PEO whose melting temperatures increase with decreasing cation size (T_m = 343, 373, and 468 K for NH_4^+, K^+, and Na^+, respectively). The admitted stoichiometry for these complexes is 4 mol of PEO monomer unit for 1 mol of cation.[8,10] The high melting temperature of the PEO·NaSCN complex together with its observed stability upon melt recrystallization were the major reasons for investigating the present system. The materials were studied under the form of films pre-

0024-9297/83/2216-0665$01.50/0